Optimal Drug Synergy in Antimicrobial Treatments

Joseph Peter Torella[1,2], Remy Chait[1], Roy Kishony[1,3]*

1 Department of Systems Biology, Harvard Medical School, Boston, Massachusetts, United States of America, 2 Department of Physics, University of Oxford, Oxford, United Kingdom, 3 School of Engineering and Applied Sciences, Harvard University, Cambridge, Massachusetts, United States of America

Abstract

The rapid proliferation of antibiotic-resistant pathogens has spurred the use of drug combinations to maintain clinical efficacy and combat the evolution of resistance. Drug pairs can interact synergistically or antagonistically, yielding inhibitory effects larger or smaller than expected from the drugs' individual potencies. Clinical strategies often favor synergistic interactions because they maximize the rate at which the infection is cleared from an individual, but it is unclear how such interactions affect the evolution of multi-drug resistance. We used a mathematical model of *in vivo* infection dynamics to determine the optimal treatment strategy for preventing the evolution of multi-drug resistance. We found that synergy has two conflicting effects: it clears the infection faster and thereby decreases the time during which resistant mutants can arise, but increases the selective advantage of these mutants over wild-type cells. When competition for resources is weak, the former effect is dominant and greater synergy more effectively prevents multi-drug resistance. However, under conditions of strong resource competition, a tradeoff emerges in which greater synergy increases the rate of infection clearance, but also increases the risk of multi-drug resistance. This tradeoff breaks down at a critical level of drug interaction, above which greater synergy has no effect on infection clearance, but still increases the risk of multi-drug resistance. These results suggest that the optimal strategy for suppressing multi-drug resistance is not always to maximize synergy, and that in some cases drug antagonism, despite its weaker efficacy, may better suppress the evolution of multi-drug resistance.

Introduction

As antibiotic-resistant pathogens become more common, clinicians increasingly turn to multi-drug treatment to control infection [1–5]. The inhibitory effect of two drugs in combination can be larger or smaller than expected from their individual effects, corresponding to synergistic or antagonistic interactions between the drugs respectively [6–9]. Synergistic interactions are usually thought of as advantageous since, for a given amount of drug, they more effectively inhibit the growth of drug-sensitive pathogens. However, *in vitro* studies have suggested that, for the same level of inhibition, more synergistic drug pairs may foster antibiotic resistance [10–12]. Antagonistic drug combinations, on the other hand, are less effective at inhibiting drug-sensitive pathogens, but can reduce and even invert the selective advantage of single-drug resistant mutants, causing selection against resistance [13].

These recent observations point to a possible tradeoff in the choice of synergistic versus antagonistic drug combinations with respect to their effects on treating infection and suppressing antibiotic resistance. However, while antagonistic drug combinations increase selection against resistance, and should therefore minimize resistance, they also kill the infection more slowly, giving resistance more time to emerge. Antagonism therefore has two contradicting effects on the evolution of resistance: on one hand, it increases the risk of resistance by decreasing antibiotic inhibition and allowing more time for resistance to evolve; on the other hand, it decreases the risk of resistance by decreasing the selective advantage of single drug resistant mutants. We ask which of these opposing effects is stronger, and therefore which type of drug interaction – synergistic or antagonistic – best prevents the overall chance of emergence of multi-drug resistance.

We frame this problem in the context of a clinical infection, formalizing the two main factors in the success of an antibiotic treatment as "treatment efficacy" and "prevention of multi-drug resistance." Treatment efficacy is the rate at which the infection is cleared by the treatment, and can be defined as the reciprocal of the time, t_{clear}, at which the total infection is eliminated, $1/t_{clear}$. Prevention of multi-drug resistance is defined as the reciprocal of the number of double-drug resistant mutants expected to arise during the course of treatment, $1/N_{double}$. In real infections, multi-drug resistance can arise either through a single mutation conferring cross-resistance to both drugs simultaneously, or through the sequential acquisition of mutations conferring resistance to each drug individually [10,14–16]. Furthermore, resistance to a single drug can develop in several small steps or in one large step [15,17–19]. For simplicity, and to emphasize the role of drug interactions, we concentrate here on an idealized case in which resistance to the two-drug combination evolves through sequential acquisition of two spontaneous mutations, each conferring strong resistance specific to one of the two antibiotics (Fig. 1).

We asked what level of drug interaction (ranging from strong synergy to strong antagonism) maximizes treatment efficacy ($1/t_{clear}$) and prevention of multi-drug resistance ($1/N_{double}$). Maximizing $1/t_{clear}$ is straightforward: as more synergistic drug

Author Summary

The use of antibiotics against bacterial infections has led to the emergence of multi-drug resistant pathogens such as tuberculosis and MRSA. In order to control resistance, clinicians have increasingly turned to multi-antibiotic therapies. The common wisdom is to use combinations of drugs that act synergistically to kill the infection, but the impact of drug synergy on the evolution of resistance is unclear. Using mathematical simulations of an *in vivo* infection model, we asked what level of drug synergy would minimize the risk of multi-drug resistance while preserving the efficacy of treatment. We found that synergy may increase or decrease the risk of multi-drug resistance in a given treatment, depending on infection properties such as mutation rate and the availability of resources. Surprisingly, under conditions of strong competition for resources within the host, we found that maximal synergy—currently favored in clinical settings—can actually increase the risk of multi-drug resistance. Our results identify conditions under which drug synergy exacerbates the problem of multi-drug resistance, and offer guidelines for the selection of drug pairs that suppress it.

Figure 1. Model of the evolution of resistance in synergistic and antagonistic drug treatments. (A) Graphical representation of model ODEs describing three bacterial subpopulations: the wild-type sensitive to both drugs (black, Eq. 1), single-drug resistant mutants (blue, Eq. 2), and double-drug resistant mutants (red, Eq. 3). Wild-type and single-drug resistant subpopulations grow with rate G (Eq. 4), mutate with rate μG and die with antibiotic killing rates $K(\tilde{D}_{WT})$ and $K(\tilde{D}_{single})$, where $\tilde{D}_{WT}$ and $\tilde{D}_{single}$ are the effective drug doses they experience, respectively (Eq. 5). We do not model the growth of the double-drug resistant strain, but simply follow the number of such mutants expected to arise via mutation. (B) The wild-type, single-drug resistant and double-drug resistant mutants experience different effective doses, $\tilde{D}$, in the multi-drug treatment. The wild-type (black bars) is affected by both the drugs and their interaction, yielding $\tilde{D}_{WT} = D(2+\varepsilon)$, where D is the dose of each of the drugs A and B (we assume the two drugs are given at the same dose) and ε is the level of their interaction ($\varepsilon > 0$, synergistic; $\varepsilon = 0$, additive; $\varepsilon > 0$, antagonistic). We assume strong resistance, such that resistant mutants are completely unaffected by the drug to which they are resistant; the effective drug dose felt by the single-drug resistant mutant is therefore that of one of the drugs alone, $\tilde{D}_{single} = D$, and is independent of ε (blue bars have a fixed value). Because double-drug resistant mutants are fully resistant to both antibiotics, they feel an effective dose of 0 (red bars). Increased synergy therefore increases killing of the wild-type, but also increases the selective advantage of the single-drug resistant mutants. Antagonistic drug pairs reduce this selective advantage, and can completely eliminate ($\varepsilon = -1$) or even invert it ($\varepsilon < -1$).
doi:10.1371/journal.pcbi.1000796.g001

pairs have increased killing potency and clear the infection more quickly, maximally synergistic drug pairs should maximize $1/t_{clear}$ [4,20]. In attempting to maximize $1/N_{double}$, however, the best choice of drug interaction is less clear. Assuming sequential acquisition of resistance to each drug, the rate at which multi-drug resistance arises will depend on the size of the single-drug resistant mutant population. The size of this single-mutant population, in turn, depends on two factors: the rate at which such mutants arise, and their selective advantage over the wild-type. Synergistic drug pairs decrease the first factor because they more quickly kill the source wild-type population from which single mutants arise. However, synergistic drug pairs also increase the second factor: single-drug resistant mutants will have a strong selective advantage in a synergistic treatment because resistance removes both the burden of one drug, and its enhancing effect on the other drug [13] (Fig. 1B). Synergistic drug pairs therefore decrease the rate at which single-drug resistant mutants appear, but increase their selective advantage. Antagonistic drug pairs do the opposite: though they allow a larger number of single-drug resistant mutants to arise, they also diminish the selective advantage of these mutants. The net effect of a given drug interaction on the evolution of multi-drug resistance is therefore not obvious, and requires a quantitative model to determine the overall impact of mutation and selection's countervailing effects.

To better understand how drug interactions affect the risk of multi-drug resistance, we used a population genetic model of microbial infection previously applied to predict single-drug resistance *in vivo* in mice [21], and modified it to account for the sequential acquisition of mutations leading to multi-drug resistance. We used this model to ask what level of drug interaction maximizes treatment efficacy ($1/t_{clear}$) and prevention of multi-drug resistance ($1/N_{double}$).

Results

Simple model for the evolution of resistance in multi-drug treatment

We based our model on work by Jumbe *et al.* [21], which investigated a mouse-thigh *P. aeruginosa* infection model [22–24]
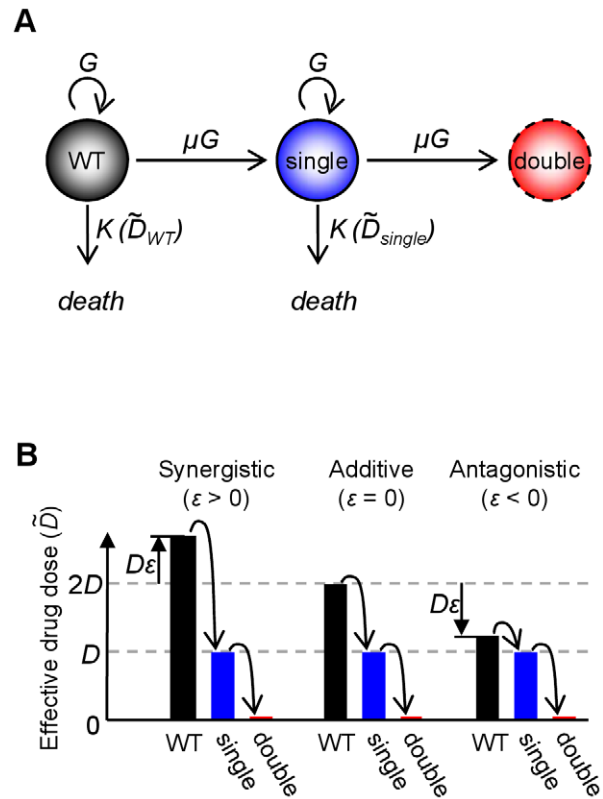
and provided a mathematical model that quantitatively described the relationship between exposure to the fluoroquinolone antibiotic levofloxacin, and changes in drug-susceptible and drug-resistant bacterial subpopulations over time. This mathematical model was successful both in reproducing the observed changes in drug-susceptible and –resistant subpopulations over time, and in predicting the dose of levofloxacin needed to suppress amplification of levofloxacin-resistant (efflux-pump-expressing) mutants. To investigate the effect of antibiotic interactions on

treatment efficacy and the prevention of multi-drug resistance in a simple scenario, we modified the Jumbe *et al.* model in four ways: we include a second antibiotic in our model; we assume a constant antibiotic dose; we assume a low hill coefficient, consistent with the mechanisms of a range of antibiotics [25]; and we assume no cost for antibiotic resistance. The consequences of these assumptions are discussed throughout the text.

Our model incorporates treatment with two antibiotics, A and B. It uses a set of ordinary differential equations (ODEs) to follow the population sizes of the drug-sensitive wild-type strain (N_{WT}), the total single-drug resistant population ($N_{single} = N_{A^R} + N_{B^R}$; we assume symmetry between drugs A and B such that their respective resistant populations are equal, $N_{A^R} = N_{B^R}$), and the expected number of multi-drug resistant mutants (N_{double}) arising over time (Fig. 1A; Methods):

$$\dot{N}_{WT} = N_{WT}\left[G - K(\tilde{D}_{WT})\right] - 2\mu G N_{WT} \quad (1)$$

$$\dot{N}_{single} = N_{single}\left[G - K(\tilde{D}_{single})\right] + 2\mu G N_{WT} - \mu G N_{single} \quad (2)$$

$$\dot{N}_{double} = \mu G N_{single} \quad (3)$$

Populations are affected by growth, antibiotic killing and mutation, where G, K and μ are the growth rate, antibiotic killing rate and frequency of resistance mutations per generation, respectively, and $\tilde{D}_{WT}$ and $\tilde{D}_{single}$ are the effective doses of antibiotic felt by the wild-type and single-drug resistant mutant populations. We assume for simplicity that antibiotic resistance imposes no fitness cost, so that the growth rates of the sensitive and resistant populations are the same. To account for competition for resources, we assume this growth rate is given by the logistic equation,

$$G = g\left(1 - \frac{N_{tot}}{N_{max}}\right), \quad (4)$$

where g is the maximal growth rate, $N_{tot} = N_{WT} + N_{single}$ is the total population size, and N_{max} is the maximal carrying capacity (Fig. S1B). This competition for resources was included in the *in vivo* murine infection model [21], and has been observed in or inferred from a range of infections [26], including *S. pneumoniae* [27], and Methicillin-Resistant *S. aureus* (MRSA) [28].

While we assume the growth rates of the wild-type and single-drug resistant mutants are the same, the rates K at which they are killed by antibiotic are different and depend on the effective antibiotic dose, $\tilde{D}$, felt by each population:

$$K(\tilde{D}) = \frac{k}{1 + \tilde{D}^{-H}} \quad (5)$$

where k is the maximal killing rate and H is the Hill coefficient, which determines the steepness of the killing rate as a function of drug dose. In contrast to Jumbe *et al.*, we set $H = 1$, which is representative of many common antibiotics [25], although different values of H give rise to similar overall model behavior (Fig. S2). The effective drug dose, $\tilde{D}$, depends on the dosage of the two drugs and on their interaction (Fig. 1B, Text S1, Fig. S1A). For simplicity we assume both drugs are administered at the same dose, D, defined in units of their minimum inhibitory concentra-

tion (**MIC**), the single-drug dose at which the wild-type death rate equals its growth rate at resource-unlimited conditions: $D_{MIC} = \left(\frac{k}{g} - 1\right)^{-1/H}$. For the wild-type, the effective dose is the sum of the dosage of the two drugs plus their level of interaction ε: $\tilde{D}_{WT} = (2 + \varepsilon)D$. Values of ε are positive, zero, or negative for synergy, additivity and antagonism, respectively. While in practice the value of ε is specific to a given drug pair [29], we treat it as continuous in order to investigate all potential treatment strategies. We assume that single-drug resistant mutants are affected by only one of the drugs, which is reasonable in the case of resistance mechanisms that decrease the intracellular concentration of antibiotic, such as efflux pump expression or enzymatic degradation [11,13,30]. The effective dose of single-drug resistant mutants is therefore $\tilde{D}_{single} = D$, and is independent of ε (Fig. 1B). Except where indicated, we set $D = 7$ MIC (general model behavior is robust to changes in drug dosage, Fig. S2A), which for an additive drug pair is consistent with the drug dosage used in Jumbe *et al.* [21].

Mutations from wild-type to single-drug resistance, or from single- to double-drug resistance, arise at a rate μ per individual per replication, or μG per individual per unit time. Since in any effective treatment the number of double mutants arising is smaller than 1, we do not account for the growth or death of this fractional population, but rather define N_{double} as the integrated number of double mutants generated via mutation during treatment (Eq. 3). Prevention of multi-drug resistance is then defined as $1/N_{double}$.

The model therefore consists of Eqs. 1–5. Parameter values, following Jumbe *et al.* [21], are given in Table S1. Initial conditions for the model are N_{WT}^0, N_{single}^0, N_{double}^0 - the population sizes at the onset of treatment. We assume that prior to treatment, the infections have grown from a single cell to the initial population size N_{tot}^0 while mutating; while the overall mutation rate is a function of model parameters μ, g and N_{max} (Eqs. 2, 3), N_{single}^0 and N_{WT}^0 are functions of μ alone: $N_{single}^0 = 2\mu N_{tot}^0$, $N_{WT}^0 = (1 - 2\mu)N_{tot}^0$. No double-drug resistant mutants are present: $N_{double}^0 = 0$. We integrate the ODEs with these initial conditions (Methods) and define t_{clear} as the time at which the total population size drops below one (t_{clear} is defined as infinity if the population reaches a non-zero steady state).

Antibiotic interactions create a saturable tradeoff between treatment efficacy and prevention of multi-drug resistance

To determine the impact of drug interaction on treatment outcome, we first looked at the differences in treatment efficacy ($1/t_{clear}$) and prevention of multi-drug resistance ($1/N_{double}$) over a range of drug interaction values ($\varepsilon = -1.5$ to 1.5) while holding drug dosage fixed (Fig. 2, $D = 7$ MIC). We observed two distinct and robust (Fig. S2) behaviors, depending on whether ε falls above or below a critical value, ε^* (Fig. 2; for the parameters used, $\varepsilon^* \approx 0.14$).

For $\varepsilon < \varepsilon^*$, we observed a tradeoff between treatment efficacy and prevention of resistance. In this regime, increasing synergy yields greater $1/t_{clear}$ (Fig. 2, unshaded region); this is expected, as increasing the synergistic interaction between the drugs kills the wild-type more quickly. Despite faster infection clearance, however, greater synergy actually decreases $1/N_{double}$; namely, it increases the risk of multi-drug resistance. Conversely, more antagonistic drug pairs increase $1/N_{double}$, albeit at the expense of reduced efficacy.

This tradeoff between efficacy and prevention of resistance breaks down at a critical threshold, ε^*, above which increasing synergy no longer increases $1/t_{clear}$, but still decreases $1/N_{double}$ (Fig. 2, shaded region). Above this "synergy ceiling," further increasing synergy therefore has only undesirable effects, since it
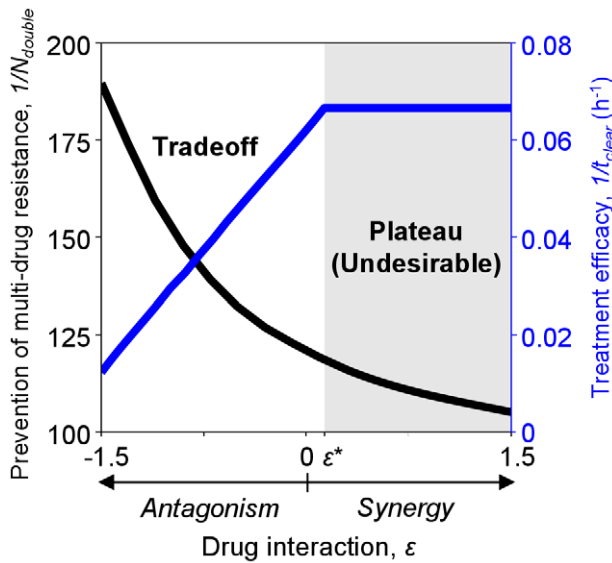
Figure 2. Choice of drug interaction presents a tradeoff between treatment efficacy and prevention of multi-drug resistance. Below a critical level of drug interaction (unshaded region, $\varepsilon < \varepsilon^*$), treatment efficacy ($1/t_{clear}$, blue) and prevention of multi-drug resistance ($1/N_{double}$, black) exhibit a tradeoff: increased synergy yields higher efficacy, but at the expense of lower resistance prevention. Above ε^*, however, efficacy plateaus: increasing synergy beyond this 'synergy ceiling' fails to improve treatment efficacy, but continues to diminish resistance prevention (shaded region, $\varepsilon > \varepsilon^*$).
doi:10.1371/journal.pcbi.1000796.g002

increases the risk of multi-drug resistance without increasing efficacy. Optimal drug pairs for treating the given infection must therefore have a level of drug interaction lower than ε^* and, due to the tradeoff between $1/t_{clear}$ and $1/N_{double}$, the optimal value of ε will depend on the relative importance assigned to these two conflicting goals.

The frequency of resistance mutations determines the "synergy ceiling" ε^*

To understand what determines the level of the synergy ceiling, ε^*, we asked what causes the transition from tradeoff behavior at $\varepsilon < \varepsilon^*$, to plateau behavior at $\varepsilon > \varepsilon^*$ (Fig. 2). Due to the sharp biphasic behavior of efficacy ($1/t_{clear}$) around ε^*, we looked to population time courses to determine how the time of clearance, t_{clear}, was affected by drug interactions below, at or above ε^* ($\varepsilon = -1.5, 0.14, 1.5$, respectively; Fig. 3A). For $\varepsilon < \varepsilon^*$ (Fig. 3A, top), the wild-type subpopulation outlives the single-drug resistant mutants and $t_{clear} = t_{clear}^{WT}$. Since wild-type killing is stronger for more synergistic drug pairs, increasing ε decreases t_{clear}^{WT}, explaining why efficacy increases with ε in this region (Fig. 2, unshaded region). For $\varepsilon > \varepsilon^*$ (Fig. 3A; bottom), however, the wild-type is eliminated before the single-mutant population, and $t_{clear} = t_{clear}^{single}$. Because the killing rate of the single-drug resistant mutants is independent of ε, t_{clear}^{single} is effectively independent of ε, causing $1/t_{clear}$ to plateau for $\varepsilon > \varepsilon^*$ (Fig. 2, shaded region). ε^* is therefore the level of drug interaction for which wild-type and single-mutant populations are cleared simultaneously ($t_{clear}^{WT} = t_{clear}^{single}$; Fig. 3A, middle).

Since ε^* represents the level of drug interaction for which $t_{clear}^{WT} = t_{clear}^{single}$, parameters that differentially alter t_{clear}^{WT} and t_{clear}^{single} will alter ε^*. While we found that a number of model parameters had some effect on ε^* (Fig. S2), the strongest effect was due to changes in the frequency of resistance mutations, μ. μ differentially affects

t_{clear}^{WT} and t_{clear}^{single} because, although it has virtually no effect on t_{clear}^{WT}, the single-mutant population size at the onset of treatment increases linearly with μ, $N_{single}^0 = 2\mu N_{tot}^0$, thereby increasing t_{clear}^{single}. For t_{clear}^{WT} to match this increase in t_{clear}^{single}, the wild-type killing rate must decrease; namely, ε^* must be reduced. We therefore expected ε^* to decrease with increasing μ and, indeed, increasing the frequency of resistance mutations gave rise to consistent decreases in ε^* (Fig. 3B). Interestingly, for high frequencies of resistance ($\mu > 2 \times 10^{-6}$) the synergy ceiling ε^* falls below zero (representing an antagonistic drug interaction); in this case mildly synergistic and even additive interactions fall in the undesirable regime where the risk of multi-drug resistance increases without any corresponding gain in treatment efficacy.

Competition for resources underlies the tradeoff between treatment efficacy and prevention of multi-drug resistance

Why does synergy, despite clearing the infection faster, increase the risk of multi-drug resistance (Fig. 2)? Since synergistic drug pairs clear the infection more quickly than antagonistic drug pairs, the rate at which they generate double mutants must also be higher. The overall rate at which double mutants arise, $\dot{N}_{double} = \mu G N_{single} = \mu g N_{single}\left(1 - \frac{N_{tot}}{N_{max}}\right)$ (Eqs. 3, 4), is affected by two variables: it increases with the size of the single-mutant population, N_{single}, and decreases with total population size, N_{tot}, due to the inhibitory effect of resource limitation on growth and mutation (Fig. 4A). The total number of double mutants expected to arise is simply the integral of this instantaneous rate over the treatment course. In order to determine why synergistic treatments increase $\dot{N}_{double}$, we therefore analyzed the trajectories of synergistic and antagonistic treatments through the space of N_{single} versus N_{tot} (Fig. 4A; $\varepsilon = 1.5$, solid line, $\varepsilon = -1.5$, dashed line). The initial slopes of these trajectories (Fig. 4A, arrows) are determined by the relative fitness of the wild-type and single-drug resistant populations under antibiotic treatment. The synergistic treatment selects strongly against the wild-type population, producing a trajectory with a steep slope that drives treatment into a region of high $\dot{N}_{double}$ (Fig. 4A, red region); this is because the rapid decrease in wild-type population size relieves competition for resources, creating a window of opportunity in which the still-large single-mutant population can rapidly grow and mutate. Conversely, the antagonistic treatment selects only weakly against the wild-type, producing a trajectory with a shallow slope that skirts the high $\dot{N}_{double}$ region. Antagonistic drug pairs therefore decrease $\dot{N}_{double}$ in a competition-dependent fashion: weak killing of the wild-type maintains competition for resources, limiting growth and mutation of the single-drug resistant population until it is eliminated.

It is important to note that resource competition is significant only at the beginning of treatment, when $N_{tot} \approx N_{max}$. If competition for resources is required for the advantage of antagonism over synergy in preventing resistance, then we should expect a decrease in initial population size to decrease this advantage. To test this prediction, we looked at the relative ability of our representative synergistic ($\varepsilon = 1.5$) and antagonistic ($\varepsilon = -1.5$) drug pairs to prevent multi-drug resistance, $t_{clear}^{ant}/t_{clear}^{syn}$, over a range of N_{tot}^0 (Fig. 4C, circles; sensitivity to other model parameters is minimal, Fig. S2). Indeed, we found that the advantage of antagonistic drug pairs in preventing resistance ($t_{clear}^{ant}/t_{clear}^{syn} < 1$, below dashed line) was limited to cases where N_{tot}^0 is close to N_{max}. In fact, for N_{tot}^0 significantly lower than N_{max}, the trend reverses and synergy better prevents resistance ($t_{clear}^{ant}/t_{clear}^{syn} > 1$, above dashed line). This is because, for low population sizes, resource competition effects are negligible; $\dot{N}_{double}$ therefore no longer depends on N_{tot}, and becomes a
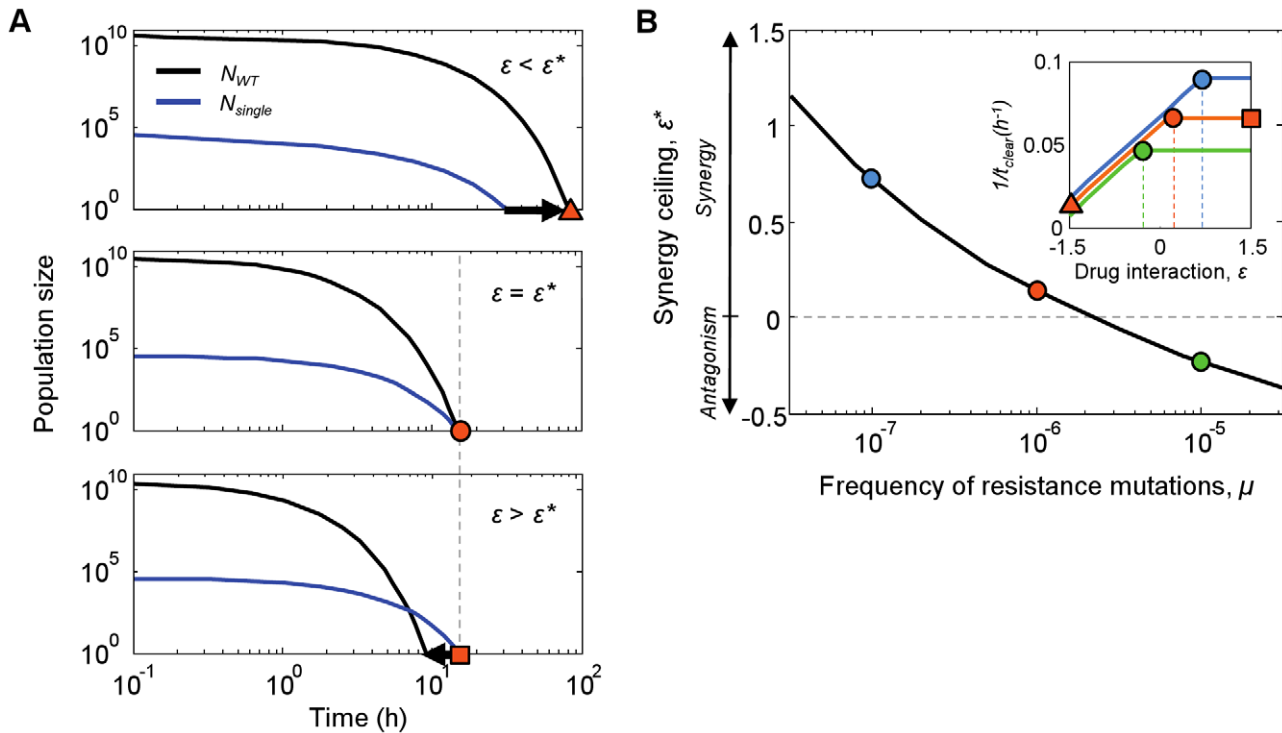
Figure 3. The synergy ceiling ε^* is determined by clearance of the wild-type population before the single-mutant subpopulation. (A) Population sizes of the wild-type (N_{WT}, black) and single-drug resistant mutants (N_{single}, blue) over treatment courses with levels of interaction below, at or above the critical value ε^* ($\varepsilon = -1.5, 0.14, 1.5$). Populations start with sizes N_{WT}^0, N_{single}^0 and are killed by antibiotics until they are cleared at times t_{clear}^{WT} and t_{clear}^{single} respectively; the overall time of clearance of the infection is simply $t_{clear} = \max\left(t_{clear}^{WT}, t_{clear}^{single}\right)$ (orange markers). The interaction level ε affects the order in which the wild-type and the single-drug resistant subpopulations are eliminated: below the synergy ceiling ($\varepsilon < \varepsilon^*$, top), the wild-type is eliminated after the single-drug resistant mutant and $t_{clear} = t_{clear}^{WT}$; at the synergy ceiling ($\varepsilon = \varepsilon^*$, middle), the two populations die simultaneously and $t_{clear} = t_{clear}^{WT} = t_{clear}^{single}$; above the synergy ceiling ($\varepsilon > \varepsilon^*$, bottom), the single-drug resistant mutant outlives the wild-type, such that $t_{clear} = t_{clear}^{single}$. Because increasing ε increases the wild-type killing rate but has no effect on the single-mutant killing rate, efficacy increases with ε below the synergy ceiling ($t_{clear} = t_{clear}^{WT}$), but plateaus at and above it ($t_{clear} = t_{clear}^{single}$; vertical dashed line: notice that $t_{clear} = t_{clear}^{single}$ is the same both at and above the synergy ceiling). (B) Increased mutation rates, μ, give rise to lower ε^*. Inset: treatment efficacy, $1/t_{clear}$, plateaus at lower levels of drug interaction ε for higher mutation rates ($\mu = 10^{-7}$, blue; $\mu = 10^{-6}$, orange; $\mu = 10^{-5}$, green; blue and green lines are shifted slightly along y-axis for clarity); ε^* values for each line are indicated by vertical dashed lines, and by circles in the main panel. Orange markers indicate the treatment efficacy achieved for different values of ε when $\mu = 10^{-6}$, corresponding to the t_{clear} values in panel A.
doi:10.1371/journal.pcbi.1000796.g003

function of N_{single} alone. Because synergistic drug pairs better limit N_{single} by quickly killing the wild-type population from which single mutants arise, they therefore also better limit multi-drug resistance in cases of weak competition. Indeed, this advantage of synergy disappeared entirely when we artificially turned off wild-type to single-mutant mutation, allowing only those single mutants present at the start of treatment to contribute to $\dot{N}_{double}$ (Fig. 4C, triangles).

Importantly, when competition for resources is weak (N_{tot}^0 significantly less than N_{max}, $t_{clear}^{ant} > t_{clear}^{syn}$), the tradeoff between treatment efficacy and prevention of multi-drug resistance no longer exists (Fig. 4D; compare with Fig. 2). As a result, ε^* is no longer useful as a "synergy ceiling" because, although drug pairs with $\varepsilon > \varepsilon^*$ do not further improve $1/t_{clear}$, they do improve $1/N_{double}$. For infections with weak competition, the use of maximally synergistic drug pairs therefore represents the best possible treatment strategy.

Discussion

We used a population dynamic model of bacterial infection to determine what drug interactions best suppress the emergence of

multi-drug resistance. Whereas antagonistic drug pairs kill bacterial populations more slowly, and therefore allow more time for resistance to emerge, they also decrease the selective advantage of resistant mutants. Which of these two opposing effects of antagonism dominates in determining its overall impact on the chance of evolving multi-drug resistance? Framing this problem in the context of a clinical infection, we asked how two measures of treatment outcome, treatment efficacy and prevention of multi-drug resistance, depend on drug interaction.

We found that the optimal drug interaction can be determined primarily as a function of two infection parameters: population size at the outset of treatment, and the frequency of resistance mutations (see summary of our results in Fig. S3). For clinically relevant scenarios where initial population sizes are well below the carrying capacity, competition for resources is weak and synergy, which is typically preferred in clinical settings for its superior treatment efficacy [3,4,20], is also expected to best prevent the emergence of multi-drug resistance.

Where resource competition is significant, however, strong synergy may not always be the optimal treatment strategy. Real infections frequently exhibit competition, due either to a scarcity of
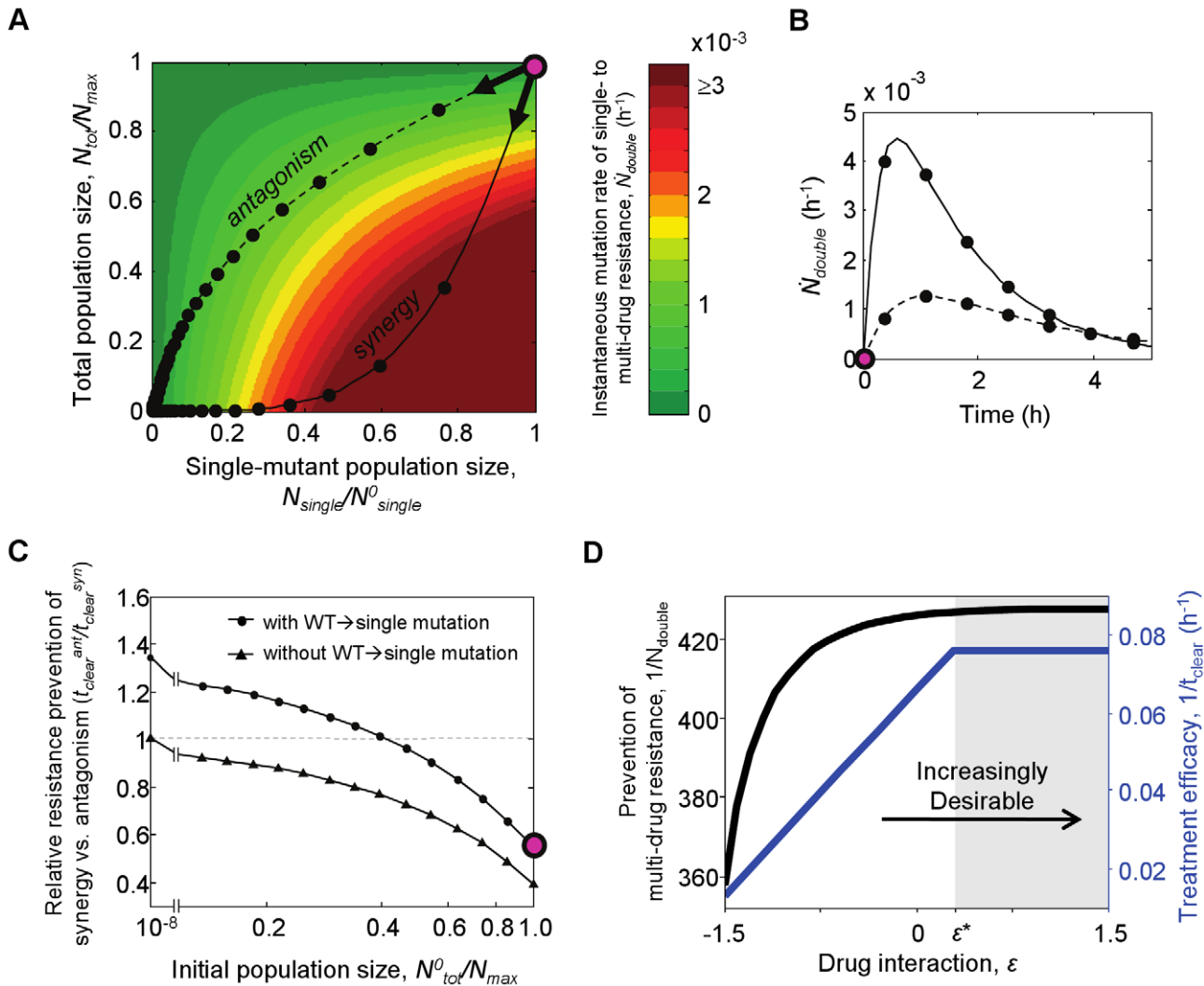
Figure 4. Prevention of multi-drug resistance by drug antagonism depends on resource competition. (A) Heat map of instantaneous rates of double-mutant formation, $\dot{N}_{double}$, as a function of single-mutant and total population sizes: $\dot{N}_{double}$ increases with the size of the single-mutant population, and decreases with total population size due to resource competition. Treatment course trajectories for synergistic ($\varepsilon = 1.5$, solid line) and antagonistic ($\varepsilon = -1.5$, dashed line) drug treatments begin with total initial population size $N^0_{tot} = N_{max}$ and initial single-mutant population size $N^0_{single} = 2\mu N_{max}$ (magenta circle), and move toward the origin as the infection is cleared (black circles indicate 20-minute intervals). The different initial slopes of these trajectories (arrows), determined by the relative fitness of the wild-type and single-drug resistant mutants in synergistic versus antagonistic treatments, lead them to different regions of the heat map: synergistic drug pairs quickly kill the wild-type, relieving resource competition before the single-mutant population is killed and leading to a region with high $\dot{N}_{double}$ (solid trajectory goes through red region), while antagonistic pairs kill the single mutants before competition is relieved, leading to a region of low $\dot{N}_{double}$ (dashed trajectory goes through green region). (B) The $\dot{N}_{double}$ over each treatment plotted as a function of time; black circles indicate 40-minute intervals in this panel. (C) Relative ability of these strongly synergistic and antagonistic drug pairs to prevent multi-drug resistance, $t^{ant}_{clear}/t^{syn}_{clear}$, for different initial population sizes (circles). For strong resource competition at the start of treatment (N^0_{tot} close to N_{max}), antagonistic drug pairs prevent resistance better than synergistic drug pairs ($t^{ant}_{clear}/t^{syn}_{clear} < 1$). For weak competition, however (N^0_{tot} significantly less than N_{max}), synergistic drug pairs better prevent resistance ($t^{ant}_{clear}/t^{syn}_{clear} > 1$). Artificially turning off wild-type to single-drug resistant mutation during treatment (leaving only the single-mutant population that exists at the onset of treatment) eliminates the advantage of synergy over antagonism at low N^0_{tot} (triangles). (D) When initial population size is low and synergy is advantageous, the tradeoff between treatment efficacy and prevention of multi-drug resistance is eliminated, such that maximally synergistic drug pairs yield both the greatest treatment efficacy and greatest prevention of multi-drug resistance (compare panel C to Fig. 2).
doi:10.1371/journal.pcbi.1000796.g004

carbon or iron [26,31,32], or saturation of available adhesion sites (e.g. in biofilm formation [33,34]). In our model, such competition is predicted to give rise to a tradeoff between treatment efficacy and resistance prevention: increased synergy leads to greater efficacy, but at the expense of an increased risk of multi-drug resistance. Importantly, this tradeoff saturates for levels of synergy greater than a critical value ε^*, above which greater synergy does not further increase efficacy, but still increases the risk of multi-

drug resistance. If the goal is to minimize multi-drug resistance, then choosing drug interactions above this "synergy ceiling" may be counterproductive. This is especially important given the dependence of ε^* on the frequency of resistance mutations: our model predicts that for infections where resistance rates are high ($\mu > 2 \times 10^{-6}$) ε^* may be negative (antagonistic), favoring the use of antagonistic drug pairs over mildly synergistic or even purely additive antibiotic combinations. Indeed, for the modified Jumbe

et al. model that we study, ε^* is nearly additive; and while the resistance frequency we use may be an overestimate (Jumbe *et al.* determined this as the rate of all mutations conferring only a 3-fold increase in the MIC), these and higher mutation rates have been identified in human pathogens [35,36]. Together, the potential for strong competition and high mutation rates in infection suggest that the tradeoff and synergy ceiling behaviors observed in our model – as well as the ability of antagonistic drug pairs to minimize multi-drug resistance – may describe the properties of some clinical infections.

We emphasize that drawing concrete therapeutic conclusions from this study would be beyond its scope. Our model incorporates many simplifying assumptions: we assume ε to be a fixed value, although it has been observed to change with both the absolute and relative doses of the antibiotics administered [37,38]; drug administration and pharmacokinetics are not considered, although they may significantly impact the evolution of resistance [23,39–42]; resistance mutation rates per generation are assumed to be independent of growth and antibiotic-killing rates; and while we consider an idealized case in which multi-drug resistance arises from strong, sequential mutations conferring resistance to each antibiotic, real mutations may confer cross-resistance to both drugs simultaneously, or only partial resistance to a single drug [10,14,16]. One consequence of partial resistance is antibiotic killing of drug-resistant mutants for drug interactions above ε^*; while for strong resistance this killing would be minimal, weak resistance may allow enough killing to undermine synergy ceiling behavior (Fig. S4). Finally, we note that this model does not consider the impact of host immune defenses, which may substantially impact microbial growth and death rates in clinical infections [43,44]; whether the influence of host defenses favors the use of some drug combinations over others, however, remains to be seen.

While these caveats indicate the limitations of this simple model and suggest important avenues for future study, our results make a number of novel predictions about the relationship between drug interaction and multi-drug resistance: that there exist conditions under which antagonistic drug pairs may better prevent multi-drug resistance despite their weaker efficacy; that there is a synergy ceiling to how much efficacy can be achieved by modulating drug interaction; and that, below this ceiling, changes in drug interaction may produce a tradeoff between inhibition and multi-drug resistance. By basing our model on a previous experimental model of infection [21], we have identified regions of parameter space in which such behaviors may be relevant in a clinical scenario, and which could be tested in future experimental models of infection. Finally, our model highlights the idea that the optimal choice of drug pair in treating an infection may be contextual: while strongly synergistic drug pairs seem the preferred strategy in scenarios where resource limitation and other forms of competition are negligible, antagonistic drug pairs may best prevent resistance in cases of high mutation rates and strong intra-infection competition. While present therapeutic knowledge generally favors synergistic drug pairs, our work motivates further research into the impact and potential utility of antagonistic interactions both in clinical and in ecological settings.

Methods

Model details

Our model consists of 3 ODEs (Eq. 1–3) describing the population sizes of the wild-type and single-drug resistant mutants (N_{WT}, N_{WT}), as well as the number of double mutants expected to arise during a treatment course (N_{double}). Parameter values for this

model include first-order maximal growth (g) and death rate (k) constants, carrying capacity N_{max} and mutation rate μ (per individual per generation), which were taken from the *in vivo* murine model investigated in Jumbe *et al.* [21] (Table S1). Initial population sizes (N_{WT}^0, N_{single}^0) were determined by assuming that, prior to treatment, the infections grew from a single cell to the initial population size N_{tot}^0 while mutating, such that $N_{single}^0 = 2\mu N_{tot}^0$ and $N_{WT}^0 = (1-2\mu)N_{tot}^0$; unless otherwise indicated, $N_{tot}^0 = N_{max}$. ODEs were solved in MATLAB (Version 7.1, MathWorks, Natick, MA) using a built-in, numerical ODE solver (ODE45). To avoid artifacts associated with using continuous ODEs to describe finite populations, each step was modified with the assumption that the wild-type or single-drug resistant population is eliminated (size decreases to zero) if its size drops below one.

Supporting Information

Figure S1 Models of drug interaction and logistic growth. (A) Model of drug interaction. The effective drug dose for the wild-type strain, $\tilde{D}_{WT}$, is a function of three variables: the doses of drugs A and B (D_A, D_B) and the interaction parameter ε (Text S1). Isoboles of the wild-type effective dose ($\tilde{D}_{WT} = 1$ MIC), are shown for additive ($\varepsilon=0$, black), synergistic ($\varepsilon>0$, red) and antagonistic ($\varepsilon<0$, blue) drug pairs. While for additive drug pairs the effective dose is a simple sum of the drugs' individual doses, synergistic or antagonistic drug pairs achieve the same effective dose with smaller or larger drug doses, respectively. All model simulations fall on the dashed line, where drug doses are equal: $D_A = D_B$. (B) Logistic growth model. As the population size, N_{tot}, increases, competition causes the growth rate, G, to fall from its maximal value, g, to 0 at the carrying capacity, N_{max} (Eq. 4). Unless otherwise indicated, in model simulations $N_{tot} = N_{max}$ at the outset of treatment (black circle).
Found at: doi:10.1371/journal.pcbi.1000796.s001 (0.11 MB TIF)

Figure S2 Prevention of resistance, and the synergy ceiling ε^*, are robust to changes in model parameters. To test the robustness of the model to parameter changes, we varied each parameter independently and measured its effect on both the relative ability of strongly synergistic and antagonistic drug pairs ($\varepsilon=1.5,-1.5$) to prevent multi-drug resistance, $\sigma_{syn}/\sigma_{ant}$ (solid black line), and the level of the synergy ceiling ε^* (solid blue line). All lines have undergone 5-point smoothing. Dashed lines indicate the points at which synergistic and antagonistic drug pairs prevent resistance equally well ($\sigma_{syn}/\sigma_{ant}=1$, black), or the synergy ceiling is additive ($\varepsilon^*=0$, blue). In each panel, those points corresponding to the original set of model parameters are indicated by circles. (A) $\sigma_{syn}/\sigma_{ant}$ and ε^* vary little with changes in drug dose D, (B) carrying capacity N_{max}, or (C) maximal growth rate g. (D) As previously discussed, increases in the frequency of resistance mutations μ decrease ε^* substantially (Fig. 3), while having no significant effect on $\sigma_{syn}/\sigma_{ant}$. (E) Likewise, increases in the initial population size, N_{tot}^0, significantly decrease $\sigma_{syn}/\sigma_{ant}$ (Fig. 4), but also decrease ε^*. (F) Changes in the Hill coefficient, H, of antibiotic killing had a more complex effect on $\sigma_{syn}/\sigma_{ant}$ and ε^*: while $\sigma_{syn}/\sigma_{ant}$ was consistently less than 1 over a wide range of H (antagonism better prevents resistance), its magnitude was parabolic with H, with antagonistic drug pairs having the greatest advantage for $H\approx3$. ε^* also appeared parabolic with H and was lowest (most antagonistic) at $H\approx2$. In the limit of large H, maximal antibiotic killing rates are achieved for both wild-type and single-drug resistant populations, regardless of drug interaction. Synergistic and antagonistic drug pairs therefore fail to differentially impact wild-type killing rates, and $\sigma_{syn}/\sigma_{ant}=1$ at

high H (black line). Furthermore, saturation of killing rates causes t_{clear}^{WT} to be greater than t_{clear}^{single} for all values of ε; ε^* is therefore undefined for $H > 3$ (blue line), though saturation of the wild-type killing rate still causes efficacy to effectively plateau for low values of ε.

Found at: doi:10.1371/journal.pcbi.1000796.s002 (0.37 MB TIF)

Figure S3 Optimal drug interactions as a function of resistance frequency and initial population size. The contour map shows the synergy ceiling, ε^*, for a given combination of resistance mutation frequency, μ, and population size at the start of treatment, N_{tot}^0. ε^* decreases monotonically with increasing μ (as in Fig. 3), but is nearly unaffected by N_{tot}^0. The black line is a single contour above which antagonistic drug pairs prevent multi-drug resistance better than synergistic drug pairs ($\sigma_{syn}/\sigma_{ant} < 1$). Above this contour, greater synergy increases the chance of multi-drug resistance; the optimal drug interaction must therefore fall below ε^*, with its specific value depending on the priority assigned to treatment efficacy versus prevention of multi-drug resistance. Below the contour, however ($\sigma_{syn}/\sigma_{ant} > 1$), greater synergy decreases the chance of multi-drug resistance; the optimal drug interaction is therefore maximal synergy (region below the black contour is colored dark red), regardless of ε^*. The magenta circle indicates the combination of μ and N_{tot}^0 corresponding to the original set of model parameters.

Found at: doi:10.1371/journal.pcbi.1000796.s003 (0.10 MB TIF)

Figure S4 Partial antibiotic resistance weakens synergy ceiling behavior. In the model we assume strong antibiotic resistance, such that the antibiotic-resistant subpopulation feels the effect of only a single drug; effectively, this makes the MIC of the drug to which it is resistant infinite and produces the familiar synergy ceiling, in which efficacy increases with ε up to a critical level ε^* and plateaus above it (blue line, Fig. 2; all lines have been shifted on the vertical axis for clarity). As previously discussed (Fig. 3), this plateau is due to the resistant subpopulation dying after the wild-type when $\varepsilon > \varepsilon^*$. When we weaken the assumption of strong resistance, however (MIC$< \infty$), drug interactions still affect drug-resistant mutants, even when such mutants are killed after the wild-type. This results in efficacy increasing over all ε, but retaining its characteristic biphasic profile (red, green, orange lines). This biphasic behavior is due to the stronger killing of the wild-type than the resistant mutant, which persists even with only partial resistance. While stronger resistance produces behavior similar to the typical synergy ceiling (MIC increases 100-fold, red line), weaker resistance (MIC increases 4-fold, orange line) yields a still-biphasic curve, but one in which increases in ε improve efficacy substantially in all cases. The synergy ceiling behavior is therefore most relevant in cases of strong antibiotic resistance.

Found at: doi:10.1371/journal.pcbi.1000796.s004 (0.08 MB TIF)

Table S1 Parameters used in this study.
Found at: doi:10.1371/journal.pcbi.1000796.s005 (0.03 MB DOC)

Text S1
Found at: doi:10.1371/journal.pcbi.1000796.s006 (0.02 MB DOC)

References

1. Levy SB, Marshall B (2004) Antibacterial resistance worldwide: causes, challenges and responses. Nat Med 10: S122–S129.
2. Golan DE, Tashjian AH, Armstrong EJ, Armstrong AW, eds. (2005) Principles of Pharmacology: The Pathophysiologic Basis of Drug Therapy. Philadelphia: Lippincott Williams & Wilkins.
3. Pillai SK, Moellering RC, Eliopoulos GM (2005) In: Lorian V, ed. Antibiotics in Laboratory Medicine. Philadelphia: Lippincott Williams & Wilkins. pp 365–440.
4. Rybak MJ, McGrath BJ (1996) Combination antimicrobial therapy for bacterial infections - Guidelines for the clinician. Drugs 52: 390–405.
5. Fitzgerald JB, Schoeberl B, Nielsen UB, Sorger PK (2006) Systems biology and combination therapy in the quest for clinical efficacy. Nat Chem Biol 2: 458–466.
6. Loewe S (1953) The problem of synergism and antagonism of combined drugs. Arzneimittel-Forschung-Drug Research 3: 285–290.
7. Berenbaum MC (1989) What is synergy? Pharmacol Rev 41: 93–141.
8. Greco WR, Bravo G, Parsons JC (1995) The search for synergy - a critical review from a response-surface perspective. Pharmacol Rev 47: 331–385.
9. Keith CT, Borisy AA, Stockwell BR (2005) Multicomponent therapeutics for networked systems. Nat Rev Drug Discov 4: 71–78.
10. Michel JB, Yeh PJ, Chait R, Moellering RC, Kishony R (2008) Drug interactions modulate the potential for evolution of resistance. Proc Natl Acad Sci U S A 105: 14918–14923.
11. Hegreness M, Shoresh N, Damian D, Hartl D, Kishony R (2008) Accelerated evolution of resistance in multidrug environments. Proc Natl Acad Sci U S A 105: 13977–13981.
12. Klein M, Schorr SE (1953) The role of bacterial resistance in antibiotic synergism and antagonism. J Bacteriol 65: 454–465.
13. Chait R, Craney A, Kishony R (2007) Antibiotic interactions that select against resistance. Nature 446: 668–671.
14. Sanders CC, Sanders WE, Goering RV, Werner V (1984) Selection of multiple antibiotic-resistance by quinolones, beta-lactams, and aminoglycosides with special reference to cross-resistance between unrelated drug classes. Antimicrob Agents Chemother 26: 797–801.
15. Mwangi MM, Wu SW, Zhou YJ, Sieradzki K, de Lencastre H, et al. (2007) Tracking the in vivo evolution of multidrug resistance in Staphylococcus aureus by whole-genome sequencing. Proc Natl Acad Sci U S A 104: 9451–9456.
16. Cohen SP, McMurry LM, Hooper DC, Wolfson JS, Levy SB (1989) Cross-resistance to fluoroquinolones in Multiple-Antibiotic-Resistant (MAR) Escherichia coli selected by tetracycline or chloramphenicol - decreased drug accumulation associated with membrane changes in addition to OmpF reduction. Antimicrob Agents Chemother 33: 1318–1325.
17. Normark BH, Normark S (2002) Evolution and spread of antibiotic resistance. J Intern Med 252: 91–106.
18. Larder BA, Kemp SD (1989) Multiple Mutations in HIV-1 Reverse Transcriptase Confer High-Level Resistance to Zidovudine (AZT). Science 246: 1155–1158.
19. Handel A, Regoes RR, Antia R (2006) The Role of Compensatory Mutations in the Emergence of Drug Resistance. PLoS Comput Biol 2.
20. Acar JF (2000) Antibiotic synergy and antagonism. Med Clin North Am 84: 1391–1406.
21. Jumbe N, Louie A, Leary R, Liu WG, Deziel MR, et al. (2003) Application of a mathematical model to prevent in vivo amplification of antibiotic-resistant bacterial populations during therapy. J Clin Invest 112: 275–285.
22. Craig WA (1998) Pharmacokinetic/pharmacodynamic parameters: rationale for antibacterial dosing of mice and men. Clin Infect Dis 26: 1–10; quiz 11–12.
23. Craig WA. Does the dose matter?; 2001 University of Chicago Press. pp S233–S237.
24. Eagle H, Fleischman R, Levy M (1953) "Continuous" vs. "discontinuous" therapy with penicillin; the effect of the interval between injections on therapeutic efficacy. N Engl J Med 248: 481–488.
25. Regoes RR, Wiuff C, Zappala RM, Garner KN, Baquero F, et al. (2004) Pharmacodynamic functions: A multiparameter approach to the design of antibiotic treatment regimens. Antimicrob Agents Chemother 48: 3670–3676.
26. Smith VH, Holt RD (1996) Resource competition and within-host disease dynamics. Trends Ecol Evol 11: 386–389.
27. Lipsitch M, Dykes JK, Johnson SE, Ades EW, King J, et al. (2000) Competition among Streptococcus pneumoniae for intranasal colonization in a mouse model. Vaccine 18: 2895–2901.
28. Dall'Antonia M, Coen PG, Wilks M, Whiley A, Millar M (2005) Competition between methicillin-sensitive and -resistant Staphylococcus aureus in the anterior nares. J Hosp Infect 61: 62–67.
29. Yeh P, Tschumi AI, Kishony R (2006) Functional classification of drugs by properties of their pairwise interactions. Nat Genet 38: 489–494.

30. Yeh PJ, Hegreness MJ, Aiden AP, Kishony R (2009) Drug interactions and the evolution of antibiotic resistance. Nat Rev Microbiol 7: 460–466.

31. Freter R, Brickner H, Botney M, Cleven D, Aranki A (1983) Mechanisms that control bacterial populations in continuous-flow culture models of mouse large intestinal flora. Infect Immun 39: 676–685.

32. Weinberg ED, Weinberg GA (1995) The role of iron in infection. Curr Opin Infect Dis 8: 164–169.

33. Nadell CD, Xavier JB, Levin SA, Foster KR (2008) The evolution of quorum sensing in bacterial biofilms. PLoS Biol 6: 171–179.

34. Zhang TC, Fu YC, Bishop PL (1995) Competition for substrate and space in biofilms. Water Environ Res 67: 992–1003.

35. Martinez JL, Baquero F (2000) Mutation frequencies and antibiotic resistance. Antimicrob Agents Chemother 44: 1771–1777.

36. Tucker SP, Stiebel TR, Potts KE, Smidt ML, Bryant ML (1998) Estimate of the frequency of human immunodeficiency virus type 1 protease inhibitor resistance within unselected virus populations in vitro. Antimicrob Agents Chemother 42: 478–480.

37. Meletiadis J, Stergiopoulou T, O'Shaughnessy EM, Peter J, Walsh TJ (2007) Concentration-dependent synergy and antagonism within a triple antifungal drug combination against Aspergillus species: Analysis by a new response surface model. Antimicrob Agents Chemother 51: 2053–2064.

38. Rand KH, Brown P (1995) Concentration-dependent synergy and antagonism between cefoperazone and imipenem against methicillin-resistant Staphylococcus aureus. Antimicrob Agents Chemother 39: 1173–1177.

39. Lipsitch M, Levin BR (1997) The population dynamics of antimicrobial chemotherapy. Antimicrob Agents Chemother 41: 363–373.

40. Roberts JA, Kruger P, Paterson DL, Lipman J (2008) Antibiotic resistance - What's dosing got to do with it? Crit Care Med 36: 2433–2440.

41. Knudsen JD, Odenholt I, Erlendsdottir H, Gottfredsson M, Cars O, et al. (2003) Selection of resistant Streptococcus pneumoniae during penicillin treatment in vitro and in three animal models. Antimicrob Agents Chemother 47: 2499–2506.

42. Foo J, Michor F (2009) Evolution of Resistance to Targeted Anti-Cancer Therapies during Continuous and Pulsed Administration Strategies. PLoS Comput Biol 5.

43. Grant AJ, Restif O, McKinley TJ, Sheppard M, Maskell DJ, et al. (2008) Modelling within-host spatiotemporal dynamics of invasive bacterial disease. PLoS Biol 6: 757–770.

44. Wodarz D (2006) Ecological and evolutionary principles in immunology. Ecol Lett 9: 694–705.